Publ. Astron. Soc. Japan 35, 437–445 (1983)

10-GHz Observations of the Unusual Supernova Remnant CTB80 Associated with Jet-like Features

Yoshiaki SOFUE, Fumio TAKAHARA, Hisashi HIRABAYASHI,
Makoto INOUE, and Naomasa NAKAI

Nobeyama Radio Observatory, Minamimaki-mura, Minamisaku-gun, Nagano 384-13*

(Received 1983 March 9; accepted 1983 May 17)

Abstract

The unusual supernova remnant CTB80 was mapped in the radio continuum emission at 10 GHz using the high-surface accuracy 45-m telescope at the Nobeyama Radio Observatory. The map reveals a compact central core, a plateau-like ridge close to the core, and three extended ridges emerging from the central region. The radio spectrum is flat over the core and plateau, while it is steep over the extended component. It is found that the narrower, shorter, and brighter a ridge is, the flatter is the spectrum, and the spectrum steepens towards the edge along each ridge. These features are reasonably understood, if the three ridges and the plateau are jets emerging from the core which involves a stellar remnant, possibly a neutron star, injecting high-energy electrons into the jets.

Key words: Radio emission; Radio jets; Supernova remnants.

1. Introduction

Irregularly shaped supernova remnants (SNR) lacking a shell structure have been noticed in these years by their central activity which is probably due to a stellar remnant like a neutron star. CTB80 is one of the irregularly shaped SNRs, having a central radio core and jet-like features. It has been pointed out that the core source has a similar nature to Crab-like SNRs (Becker et al. 1982). CTB80 has been mapped at several radio frequencies: at 610 MHz by Angerhofer et al. (1980) and Strom et al. (1980), at 2.7 GHz by Velusamy and Kundu (1974), and at 5 and 10 GHz by Velusamy et al. (1976), although the last two observations cover only a part of the SNR. All these maps reveal a central core, a plateau-like enhancement close to the core, and an extended component which is composed of three ridges running from the center. A suggestion has been made that the ridges in the extended component are jets emerging from the core (Dickel et al. 1981).

In the present paper we report the results of 10-GHz observations of CTB80 using a newly completed high-surface accuracy 45-m telescope at the Nobeyama Radio Observatory (NRO). We present a map of the SNR covering a region as wide as $1^\circ.2 \times 1^\circ.2$, an area large enough to show the entire extended component. We obtain the spectral index distribution by comparing our data with a 2.7-GHz map of Velusamy and Kundu (1974).

* Nobeyama Radio Observatory, a branch of the Tokyo Astronomical Observatory, University of Tokyo, is a facility open for general use by researchers in the field of astronomy and astrophysics.

A brief discussion is made of the relationship of the jet-like features to the core source and of their origin.

2. Observations

Observations were made on December 2, 9, and 14, 1982 using the 45-m telescope at the Nobeyama Radio Observatory. The HPBW of the antenna was $2'.70 \pm 0'.03$. The center frequency was 10.2 GHz and the bandwidth was 500 MHz. We used a cooled parametric amplifier connected with a Dicke switch referring a cooled dummy at 20-K stage. The system noise temperature was ~ 100 K. We used a circularly polarized feed system and detected one polarization component. The total intensity was obtained by assuming that the circular polarization in the source and calibration sources are negligible. The flux density was calibrated using the radio sources 3C161 (3.3 Jy at 10.2 GHz), 3C147 (4.2 Jy), and NGC 7027 (6.5 Jy), whose fluxes were obtained by interpolation of the data given by Baars et al. (1977). The aperture efficiency of the antenna was $60 \pm 5\%$ and the conversion factor between brightness temperature and equivalent flux density per beam was $T_b/S = 0.47 \pm 0.05$ K Jy^{-1}. The error in the flux and brightness determination is approximately $\pm 7\%$, which arises mainly in the process of calibration.

We mapped a squared area of $1^\circ.2 \times 1^\circ.2$ centered on R.A. (1950) $= 19^h51^m30^s.0$ and Decl. (1950) $= 32^\circ 45'.0$. The area was scanned in the right ascension and declination directions at intervals of $1'.2$ at a scan speed of $1.2^\circ/50$ s. Four independent maps were obtained, three maps by the declination scan and one map by the right ascension scan. The observing time was 1 hr per one map and in total 4 hr. Small areas surrounding the calibration sources were mapped for the calibration of the intensity and position. The pointing accuracy was better than $0'.2$. The four maps were added to get a final map, on which the rms noise is approximately 5 mK. Data reduction was made using a radio astronomical reduction system at the NRO, a part of which contains the NOD2 reduction package described by Haslam (1974). Scanning effects, which were mainly caused by weather conditions, were removed by using the "pressing method" of Sofue and Reich (1979). The computations were made on a FACOM M200 and M180IIAD at NRO.

3. Results

The resulting map of the total intensity distribution at 10 GHz of CTB80 is shown in figure 1 in the form of a contour map. The contour interval is 16.3 mJy/beam or 7.72 mK in brightness temperature (the unit of numbers on the contours is 1.54 mK).

The entire source may be divided into three components: a central core, a plateau-like ridge, and an extended component composed of three jet-like features.

(*i*) *Compact core*: The central compact core is located at R.A. $= 19^h51^m4^s.3 \pm 0^s.8$, Decl. $= 32^\circ 44' 33'' \pm 10''$ (epoch 1950). The peak flux density over this component is 0.97 ± 0.07 Jy. After removing the plateau component, the core source has the total flux density of 0.44 ± 0.1 Jy. The core is not resolved with the present HPBW of $2'.7$. Indeed high-resolution observations of the core at 5 GHz by Angerhofer et al. (1981) showed that its extent is approximately $0'.5$. Total flux densities of the core at 610 MHz, 1400 MHz, and 5 GHz are shown to be nearly constant at ~ 500 mJy (Angerhofer et al. 1981). It is remarkable that the spectral index of the core over a wide range of frequency from 0.6 to 10 GHz is as flat as $\alpha \approx -0.05$ ($S \propto \nu^\alpha$ with S the flux density and ν the frequency; table 1).

(*ii*) *Plateau* (*P-jet*): The plateau component appears as an extension from the core towards the east. The axis of the plateau is at a position angle of $\sim 100^\circ$. An east-west

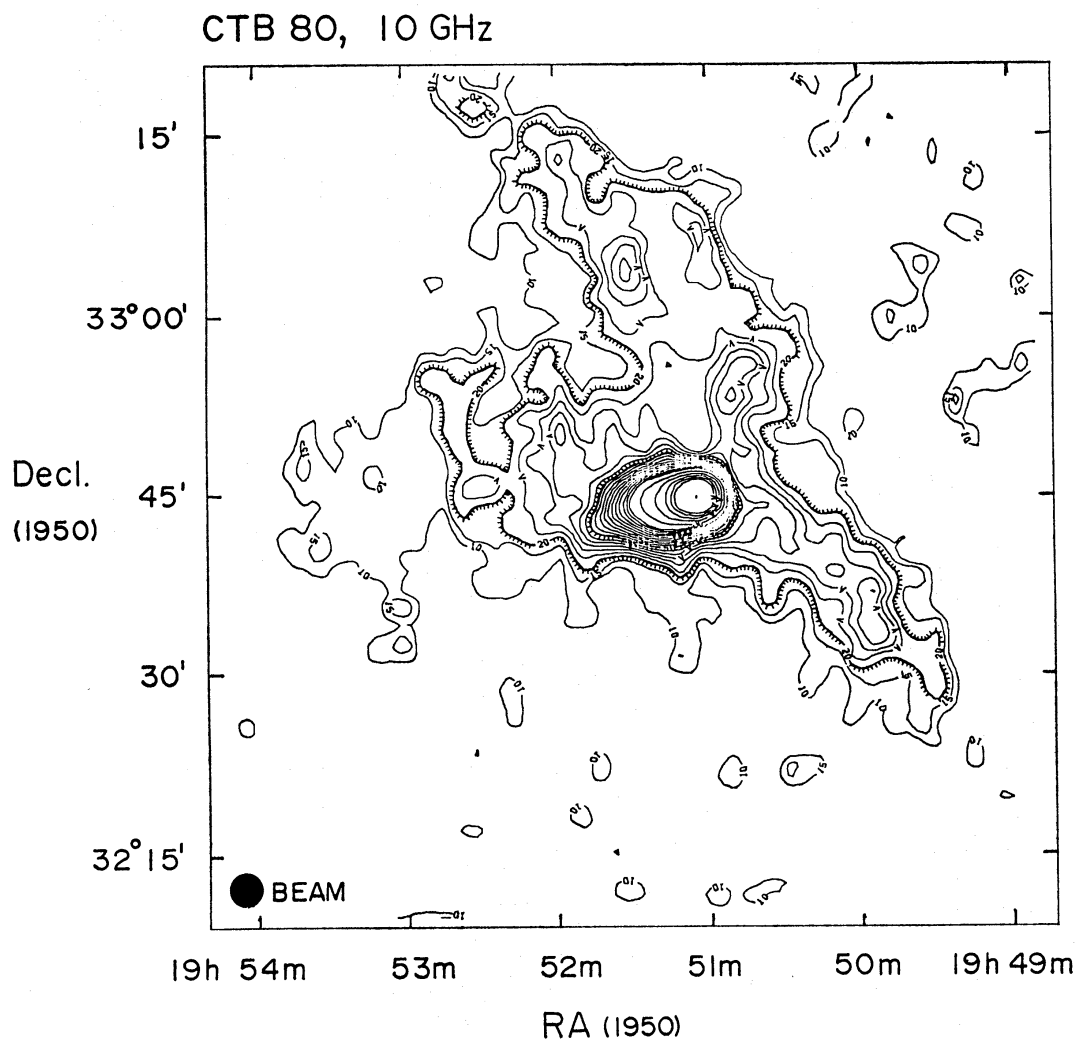

Fig. 1. A contour map of the total intensity distribution of CTB80. The contour interval is 7.72 mK in brightness temperature up to $T_b=154$ mK, and is 30.8 mK up to $T_b=308$ mK. The peak brightness temperature is 444 mK. The unit of the numbers on the contours is 1.54 mK. The map center is R.A.$=19^h51^m30^s$, Decl.$=32°45'00''$ (1950). The HPBW is 2'.7 which is indicated at the lower-left corner.

Table 1. Flux densities of the core, plateau, and extended components in CTB80, and their spctral indices.

Frequency	Core	Plateau	Extended
	Flux (Jy)		
0.61*	~0.5	2.5	—
1.4*	~0.5	—	—
5*	~0.5	—	—
10.2	0.44±0.1	1.8±0.3	16.6±1.2
	Spectral index α (0.6–10 GHz)		
	~−0.05	~−0.12	~−0.8

* Taken from Angerhofer et al. (1981).

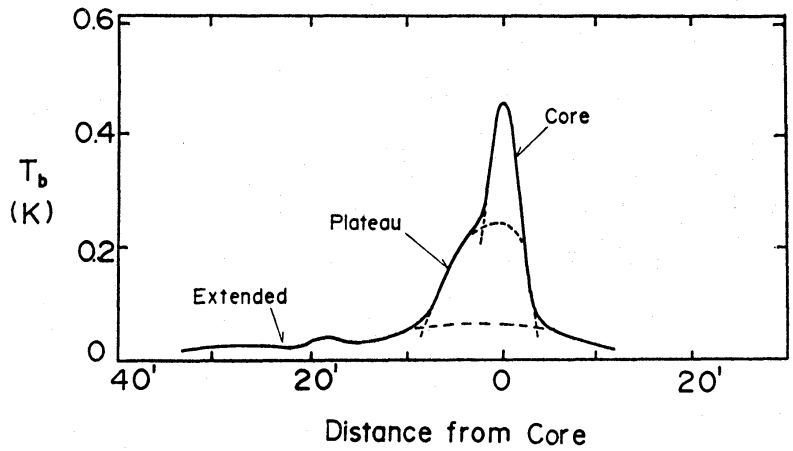

Fig. 2. An east-west crosscut of CTB80 across the central core. The source is divided into three components: the core, plateau, and extended components.

crosscut across the core is shown in figure 2 from which we can derive the extent of the component. The extent in the EW direction (distance between half-intensity points) is approximately 8!5 and the width in the NS direction is $\sim 4'$. The total flux density of this component, after removing the core, is $\sim 1.8 \pm 0.3$ Jy at 10 GHz. Combining with the flux at 610 MHz of 2.5 Jy (Angerhofer et al. 1981), we get the spectral index of $\alpha \sim -0.12$ between 0.6 and 10 GHz (table 1). The flat spectrum indicates that the plateau component is closely connected to the central core and relativistic electrons are young, if they are ejected from the core. For later convenience we may call the plateau P-jet.

(*iii*) *Extended component*: The extended component is composed of three jet-like features emerging from the central core. The northern ridge (we may call this N-jet for later convenience) emerges from the core towards the NW at a position angle of $\sim 340°$. The jet is bent towards the east at an angular distance of $\sim 12'$ from the core and reaches as far as $\sim 40'$, drawing an arc-shaped ridge. The ridge bifurcates into two parts at 15′–25′ from the core.

A south-western ridge (SW-jet) emerges from the core towards the west at a position angle of $\sim 250°$ and bends towards SW gradually, extending up to 30′ apart from the core. The ridge is again arc-shaped and is narrower than the N-jet. The mean brightness over the SW-jet is the highest among the three ridges.

The eastern ridge (E-jet) is an apparent extension of the plateau component. The E-jet is more diffuse and extended than the other ridges, reaching as far as $\sim 50'$ from the core. No sharp ridge like those of the N- and SW-jets is seen over the E-jet. On account of the discrepancy between spectral indices in the E-jet and the plateau component as discussed later, the E-jet may not be a real extension of the plateau, although its origin seems common at the core.

The entire appearance of CTB80 in our 10-GHz map is in excellent agreement with that in the 610-MHz WSRT synthesized map of Angerhofer et al. (1981) and Strom et al. (1980). On the other hand, our 10-GHz map shows a significant difference from a 10-GHz map of Velusamy et al. (1976). The present map does not show such sharp and straight ridges extending towards the east and west appearing in the map of Velusamy et al. (1976). The discrepancy may be due to a narrow coverage in the declination (10′ wide) in their observations.

(*iv*) *Flux densities*: We determined the total flux density at 10 GHz for each com-

Table 2. Characteristic properties of the jet-like features in CTB80.

Feature	Shape	Approximate extent*		Position angle	Spectral index	S_{10GHz} (Jy)	$T_{b,10GHz}$ (K)	Radio luminosity† (1–10 GHz) (erg s^{-1})
		Length	Width					
Core	Compact, round	0′.5	0′.5	—	−0.05	0.44±0.1	6±3‡	$\sim 5\times10^{31}$
P-jet	Plateau-like, straight	8′.5	∼4′	∼100°	−0.12	1.8 ±0.3	0.15 ±0.03	$\sim 2\times10^{32}$
SW-jet	Jet-like, bent, arc	∼20′	∼5′	230°–240°	−0.47±0.11	16.6 ±1.2	0.054±0.008	$\sim 3\times10^{33}$
N-jet	Jet-like, bent, arc	∼30′	∼10′	350°– 20°	−0.56±0.09		0.054±0.011	
E-jet	Diffuse, extended	∼40′	∼20′	∼90°	−0.95±0.13		0.032±0.017	

* Read from the 610-MHz map of Angerhofer et al. (1981).

† A distance of 3 kpc is assumed.

‡ A size of 0′.5×0′.5 is assumed.

Table 3. Total flux densities of CTB80.

Frequency (GHz)	Flux density (Jy)	Reference
0.61	165	Angerhofer et al. (1981)
0.75	127 ±15	Velusamy et al. (1976)
1.0	121 ±15	Velusamy et al. (1976)
1.4	80	Galt and Kennedy (1968)
2.7	42 ± 3	Velusamy and Kundu (1974)
5	31.0± 2.5	Velusamy et al. (1976)
10.2	18.8± 1.3*	Present paper
10.7	14.0± 1.4	Velusamy et al. (1976)

* The error of ±7% arises in the process of calibration.

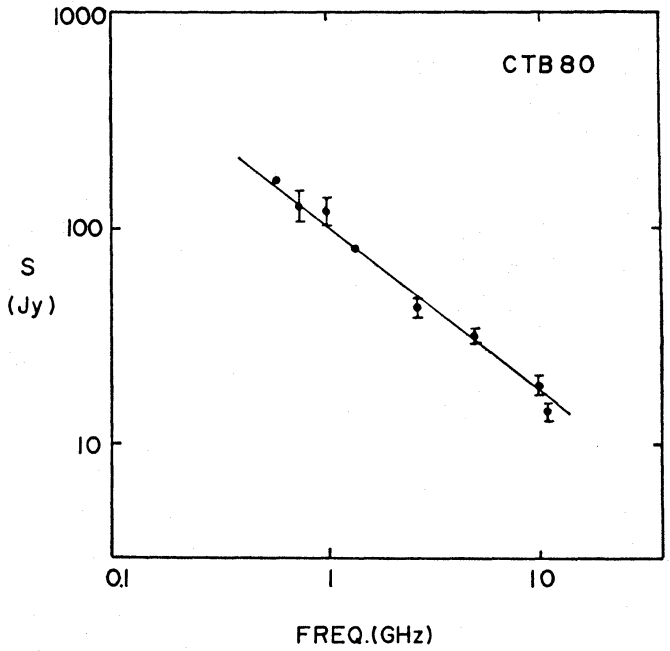

Fig. 3. Total flux densities of CTB80 plotted against the frequency. The data are from table 3. The spectrum is well fitted with a power law as indicated with the straight line which has a spectral index of $\alpha = -0.77 \pm 0.03$.

ponent from our data. The total flux density of the core is 0.44±0.1 Jy, the plateau component (P-jet) 1.8±0.3 Jy, and the extended component 16.6±1.2 Jy (table 1). Each of the N-, E-, and SW-jets shares approximately one third of the flux of the extended component. The total flux density of entire CTB80 is 18.8±1.3 Jy. The mean brightness temperature (T_b) along each ridge and those of the P-jet and core are shown in table 2.

(*v*) *Spectral indices*: Table 3 lists the total flux density of CTB80 obtained above together with those measured at different frequencies from the literature. We plot them in figure 3. The flux distribution against frequency is well fitted with a power-law spectrum of index $\alpha = -0.77 + 0.03$. The spectral index of the extended component alone, after removing the central core and plateau components, is $\alpha \sim -0.8$.

Combining our data with a 2.7-GHz filled-aperture map by Velusamy and Kundu (1974), we obtain spatial distributions of the spectral index along the ridges. The 10-GHz map was smoothed to a HPBW of 5′.5 of the 2.7-GHz map, and the smoothed 10-

GHz map was compared with the 2.7-GHz map to get the spectral index. Figure 4 shows the variation of spectral index as a function of the distance from the core along each jet of the extended component. The central region containing the core and plateau has a flat

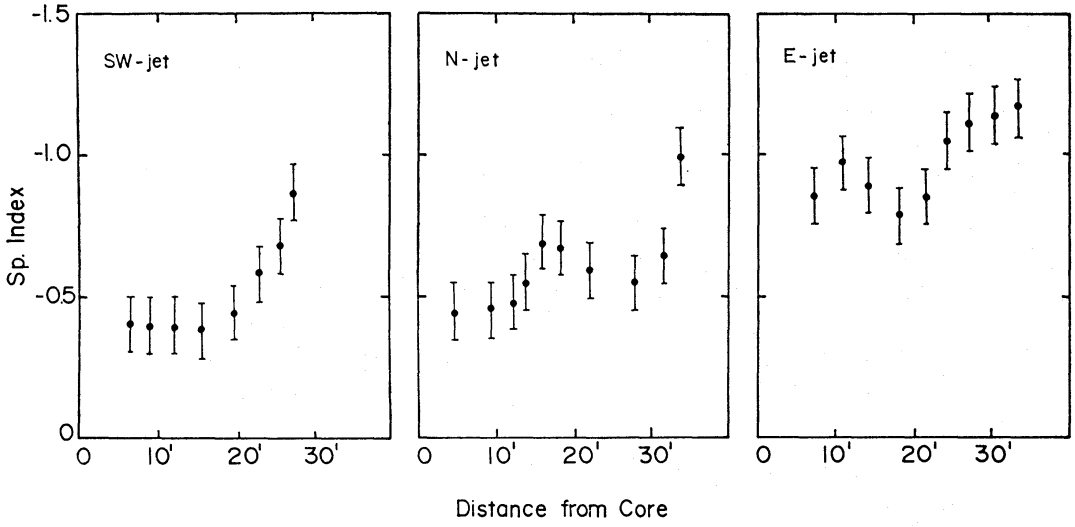

Fig. 4. Spectral index between 2.7 and 10 GHz as a function of distance from the core along each ridge in the extended component, or along the SW-, N-, and E-jets. Note the steepening of the spectrum towards the edge of a jet. The mean spectral index becomes steeper from the SW-jet to the E-jet. The indicated errors of $\sim \pm 0.1$ are mainly due to the errors on reading the brightness temperature on the 2.7 GHz map of Velusamy and Kundu (1974).

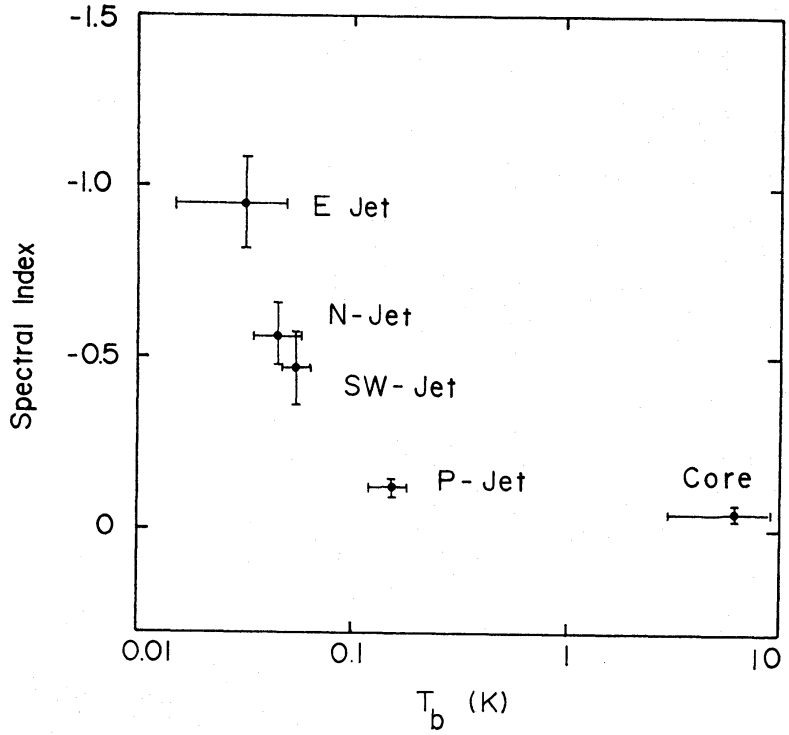

Fig. 5. Mean spectral indices plotted against mean brightness temperature of the jets and core. Note the steepening of the spectrum with decrease in the brightness temperature.

spectrum. The spectral index over the three jets in the extended component is as steep as $\alpha \sim -0.8$. However, the spectrum over the SW-jet is somewhat flatter, $\alpha = -0.47 \pm 0.11$, and then it becomes steeper in the order of the N-jet ($\alpha = -0.56 \pm 0.09$) and the E-jet (-0.95 ± 0.13) (see table 2). This implies that the narrower, shorter, and brighter a jet is, the flatter is its spectrum. This tendency holds even if we include the P-jet, which has a flat spectrum of $\alpha = -0.12$.

In figure 5 we plot the mean spectral index along the ridge of a jet against its mean brightness temperature. It is remarkable that the spectrum is steeper as the brightness decreases. We emphasize that, as figure 4 shows, the spectrum becomes steeper along each jet towards the farther position from the core. We may recall that such steepening of the spectrum along a jet is typical of extragalactic radio jets associated with active radio galaxies and quasars.

4. Discussion

The relationship of the extended component to the central core has been a question on account of its very different spectral index from that of the core and its unusual morphology. The association of the extended component was particularly difficult to understand, if the core is a "normal" Crab-like object (Becker et al. 1982). However, details in the structure appearing on the high resolution map of Angerhofer et al. (1981) rather suggest the association. The systematic variation of the spectral index as a function of the distance from the central core along the jets (figure 4) strongly indicates their physical connection to the core. The steepening of the spectrum along each jet suggests a supply of relativisitic electrons from the core.

We note that the plateau (P-jet) has also an appearance like a unidirectional jet emerging from the core. Its flat spectrum, compact size, and high radio brightness suggest an injection of material containing energetic electrons, not yet diminishing in their higher energy portion, into this plateau from the core. Namely, the P-jet may be in an early stage of a jet emerging from the core.

An X-ray image of the core was obtained using the high-resolution imager of the Einstein Observatory by Becker et al. (1982). They showed that the X-ray emission has a diffuse component with a diameter of about 30″ and that 25–30% of the total flux comes from the point source, which is taken as the clear evidence for the existence of a stellar remnant in the center of the SNR. The radio core probably owes its activity to the central star. The existence of the X-ray point source and the radio core with a flat spectrum suggests that the jets may be produced by activities in the central star.

The association of SN 1408 with this SNR (Strom et al. 1980), which gives the age of the SNR as 600 yr, has been questioned by van den Bergh (1980) on the ground of the required large ejection speed. Becker et al. (1982) has also questioned the young age on account of low X-ray and low radio luminosities. If the age of the SNR is much older, the whole jets may be ascribed to a long-lived, continuous injection of energetic particles from a powerful central star like a rotating neutron star. A further study of the stellar remnant such as a search for the binary nature and the pulsing component in the radio emission seems to be essential to clarify the problem.

References

Angerhofer, P. E., Strom, R. G., Velusamy, T., and Kundu, M. R. 1981, *Astron. Astrophys.*, **94**, 313.
Angerhofer, P. E., Wilson, A. S., and Mould, J. R. 1980. *Astrophys. J.*, **236**, 143.
Baars, J. W. M., Genzel, R., Pauliny-Toth, I. I. K., and Witzel, A. 1977, *Astron. Astrophys.*, **61**, 99.
Becker, R. H., Helfand, D. J., and Szymkowiak, A. E. 1982, *Astrophys. J.*, **255**, 557.
Dickel, J. R., Philip, E., Angerhofer, P. E., Strom, R. G., and Smith, M. D. 1981, *Vistas Astron.*, **25**, 127.
Galt, J. A., and Kennedy, J. E. D., 1968, *Astron. J.*, **73**, 135.
Haslam, C. G. T. 1974, *Astron. Astrophys. Suppl.*, **15**, 333.
Sofue, Y., and Reich, W. 1979, *Astron. Astrophys. Suppl.*, **38**, 251.
Strom, R. G., Angerhofer, P. E., and Velusamy, T. 1980, *Nature*, **284**, 38.
van den Bergh, S. 1980, *Publ. Astron. Soc. Pacific*, **92**, 768.
Velusamy, T., and Kundu, M. R. 1974, *Astron. Astrophys.*, **32**, 375.
Velusamy, T., Kundu, M. R., and Becker, R. H. 1976, *Astron. Astrophys.*, **51**, 21.